Thermal Actuation of Phase Change Tin Pump

Naagarajan Ramachandran

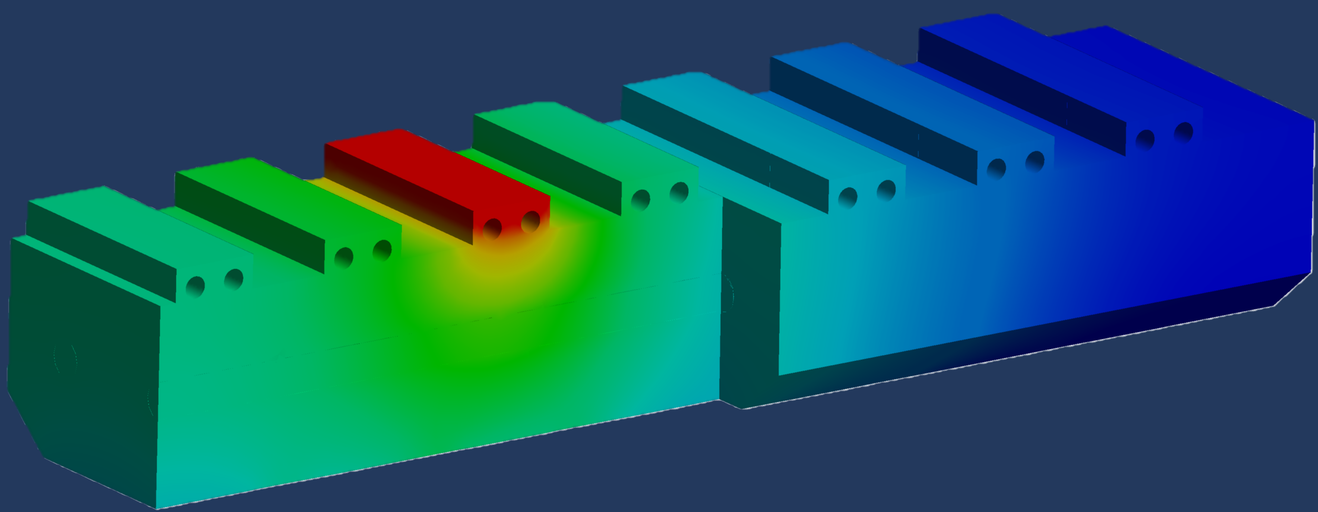

TU Delft

Thermal Actuation of Phase Change Tin Pump

Thesis

by

Naagarajan Ramachandran

to obtain the degree of Master of Science
at the Delft University of Technology
to be defended publicly on October 03, 2023 at 14:00

Thesis committee:

Chair:	Dr. Siddhant Kumar (TU Delft)
Supervisor:	Dr. *ir.* Willem Michiel de Rapper (ASML)
External examiners:	Dr. Shoshan T. Abrahami (TU Delft)
	Dr. *ir.* Luis Cutz (TU Delft)
Place:	Faculty of Mechanical, Maritime, and Materials Engineering, Delft
Project Duration:	January, 2023 - October, 2023
Student number:	5231388

An electronic version of this thesis is available at `http://repository.tudelft.nl/`.

Faculty of Mechanical, Maritime, and Materials Engineering · Delft University of Technology

Delft University of Technology

Abstract

Pressurized liquid Tin finds application in the generation of Extreme Ultra-Violet light for semiconductor lithography. In order to improve the throughput of the lithography systems, tin must be pressurized to higher levels, and in turn, new pressurization methods are needed.

A phase change tin pump is an innovative system that pressurizes and pumps liquid Tin by harnessing the expansion and contraction during phase changes, without the need for any moving parts. The pump needs to pressurize liquid tin up to 2000 bars, with a pumping capacity of 4 ml/hr. Since this system relies heavily on control over the temperatures of tin, this study is set up to address the thermal constraints in the system by investigating three aspects of temperature distribution in the system.

Firstly, the heaters in the pump are placed at discrete locations, but the working volume is continuous. Thus, it is challenging to define a temperature control function that can facilitate uniform melting and continuous flow of tin. The relation between rate of heat input to the pump and the rate of heat transfer in tin is estimated using an analytical model. From the analytical model, it is found that heating rates of the order of 0.1 K/s are required in order to melt tin in a reasonably uniform fashion over a zone length of 5 mm.

Secondly, the number of heaters are limited, and it is hard to achieve precise control over the temperature of tin at any given location. In order to establish a good basic control, the free design parameters are optimized so that a steady state gradient of 50 K is achieved between solid (200°C) and liquid (250°C) tin in the working volume. This is done by evaluating the thermal profile of the system for different combinations of the design variables, using Finite Element Analysis. The two objectives of this optimization problem (maximum temperature gain and minimum crosstalk) are seen to have contrasting requirements of the design variables. An optimal combination of the variables is found such that a gradient of 50 K is possible, but with a little trade-off on both the objectives.

Thirdly, a direct measurement of temperature of tin inside the pump is not feasible, and tin temperatures are estimated analytically. The accuracy of estimation is impacted by changes in local temperatures due to the non-linear properties of tin like absorption/release of latent heat, pressure-dependent melting point. The effect of non-linear tin properties on local temperature distribution is studied by setting up a finite difference model. It is seen that the absorption of latent heat during melting of tin results in a temperature that is 12 K lower than what would have been without the effect of latent heat.

In summary, a functional design must have:

- a heating rate of 0.1 K/s to induce uniform melting across a zone length of 5 mm
- a distance of 140 mm between heaters and a sink contact area of 45×25 mm^2 to establish good control over phase changes of tin in the pump
- a control system capable of handling a temperature retardation of 12 K in tin due to phase change

Furthermore, to improve the operational envelope of the pump, it is recommended that the following items be investigated:

- the possibility to apply higher ramp rates, and over longer zone lengths, using a more representative model of heat flow in the system
- the possibility to achieve better control over tin temperatures by dynamically adjusting both the rate of heat input and heat extraction with time
- a pump design that is optimized also for transient conditions
- studying the effect of pressurization on the temperature and phase distribution in tin, in order to improve the accuracy of estimation of tin temperatures

Acknowledgements

Thank you, Dr. *ir*. Michiel de Rapper, Thermal Architect, ASML, for the opportunity to work on this advanced technology called the phase change tin pump. As a person with a Materials Science background, doing thermal analyses with numerical methods was way out of my specialization and very challenging. Thank you for guiding me and supporting me through this project, without which this thesis would have not taken shape.

Thank you, Dr. Siddhant Kumar, Assistant Professor, Materials Science and Engineering, TU Delft, for guiding and supporting me in my graduation process.

Thanks to all members of the team – “Machine Conditioning – Tin Architecture” at ASML, who have helped me academically or administratively during my period at ASML.

Thanks to ASML for this wonderful internship opportunity. I would dearly cherish my days at ASML as working with one of the most technologically advanced, culturally diverse companies, and as a company that really stands by its core value ‘Care’.

Thanks to all my friends who have always been there for me at all times. Thanks for bringing me all the positivity I needed for the successful completion of this master’s program.

Thank you Amma & Appa for your unwavering love and support. Thank you for always being there for me. Obtaining a master’s degree would have not been possible without your encouragement and support. Where I am in my life now, I owe it all to you. And thanks to my entire big family for cheering and rooting for my success.

Thank God for blessing me with strength and courage in this endeavor.

Contents

List of Figures

List of Tables

1

Introduction - Advanced Lithography

1.1. Advanced Semiconductor Lithography

The demand for semiconductors is ever-rising, since they are used in more applications across all fields such as education, IoT, healthcare, defense, etc. In order to meet the demands, state-of-the-art lithography technology is needed to make semiconductor chips at a faster rate.

ASML makes the most advanced semiconductor lithography machines in the world, which use extreme ultra-violet (EUV) light for lithography. With EUV wavelength as small as 13.5 nm, it is possible to print features with a resolution of 3 nm. To increase semiconductor production capacity, researchers are exploring methods to increase the throughput of these lithography machines.

1.2. Extreme Ultra-Violet light source

Extreme Ultra-Violet (EUV) light is generated by ionizing small precisely-shaped droplets of ultra-pure liquid tin (refer figure 1.1). The throughput of ASML's lithography machines can be increased by increasing the intensity of the EUV light, which in turn can be increased by increasing the frequency of Tin droplet generation. However, if the distance between subsequent droplets is too small, the ionization of one droplet may affect the shape of the adjacent droplet, which is undesirable. For this reason, the distance between subsequent droplets must remain constant. To increase the droplet generation frequency while maintaining the droplet spacing, the velocity if the droplets must be scaled up proportionally.

The kinetic energy (KE) of a droplet with mass m and velocity v is given by:

$$KE = \frac{1}{2}mv^2 = PV \tag{1.1}$$

where V is the volume of the droplet and P is the pressure at which it is ejected.

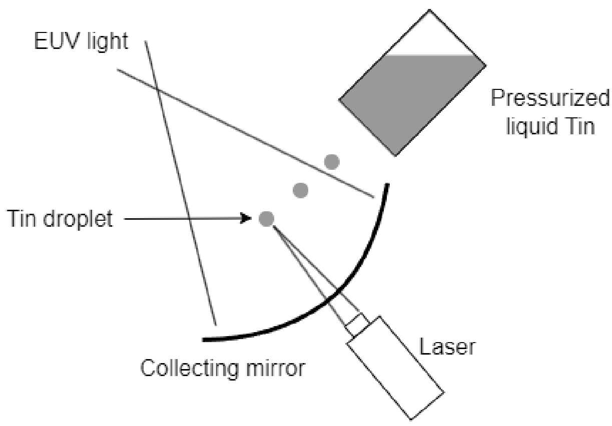

Figure 1.1: A schematic of EUV generation

At present, tin droplets are generated by pressurizing liquid tin using Argon gas up to 300 bars. To double the velocity of tin droplets ($2v$) with the same volume (V), the pressure exerted on liquid tin must be quadrupled ($4P$) (equation 1.1). To achieve pressures as high as 1200 bars (4×300) would be challenging with gas systems, due to possible liquefaction of Argon and the safety risks associated with compressed gas. Hence, other pressurization means are explored.

An innovative way to make pressurized liquid Tin is to melt tin in a rigid container of fixed volume. The arrested expansion of tin during melting results in a rise in pressure of tin. A Phase Change Tin Pump (PCTP) is a system that uses this principle to pressurize and pump liquid tin.

In Chapter 2, the working principle of the phase change tin pump is described. The operational requirements, and the constraints to meet these requirements are discussed. Focus is laid on the thermal constraints. In Chapter 3, the design of the prototype is given. Variables affecting heat flow in the system are explained. Three aspects of the thermal behavior of the system, namely, transient thermal gradient, steady state thermal gradient, and the impact of non-linear material properties on temperatures, are studied in Chapter 4, Chapter 5, Chapter 6 respectively.

2

Phase Change Tin Pump

2.1. Physics behind the pump

As the name suggests, a Phase Change Tin Pump (PCTP) is a system that pumps Tin by harnessing its phase change expansion/contraction. Tin expands by about 2.7% when it melts [1]. If it is forced to melt inside a rigid container of fixed volume, the expansion is arrested, so the pressure of tin increases instead. This results in pressurized liquid tin in the container.

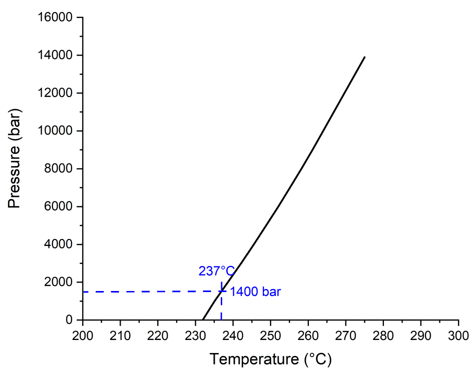

Figure 2.1: Melting curve of Tin [2]

The counter-effect is that pressure increases the melting point. The pressure-dependent melting point of tin is captured in the melting curve (figure 2.1. Using the melting curve, one can also estimate the maximum rise in pressure on melting due to suppressed expansion. From figure 2.1, it can be seen that a rise in temperature of just 5°C above the melting point (231.92°C) pressurizes tin upto 1400 bars (assuming that the container is perfectly rigid and liquid tin is perfectly incompressible). Using this effect, it is possible to create a continuous supply of pressurized liquid tin.

2.2. Pump Cycle

Consider a hollow tube filled with Tin as shown in figure 2.2 (a). One end of the tube is connected to a high pressure tin container, and this end is assumed to act as a rigid container. When a small amount of Tin is melted at this end (figure 2.2(b)), it gets pressurized since it cannot expand in the fixed volume of the rigid container. It is assumed that the solid block of Tin forms one of the walls of the rigid container, and is not pushed away by the pressure of the liquid tin. The other end of the tube is connected to a liquid tin reservoir.

When more tin is melted at the high pressure end of the tin block, it expands and adds to the pressure. Meanwhile, when more tin is solidified at the low pressure end, it contracts (figure 2.2 b&c). If this process is repeated, tin is technically pumped from the low pressure to the high pressure end, while the solid tin block moves in the opposite direction.

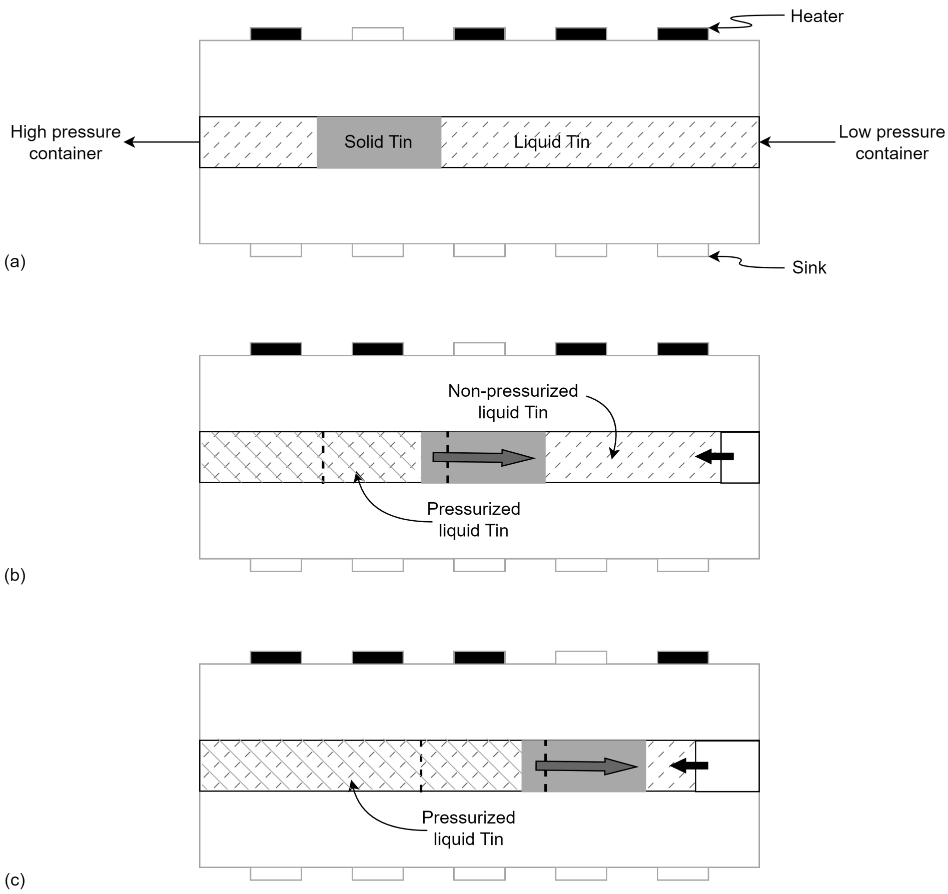

Figure 2.2: Conceptual pump cycle

2.3. Requirements

The high level requirements for this pump to be more efficient than the gas pressurized system are:

1. Liquid tin must be pressurized to 2000 bar in order to generate droplets at about twice the velocity
2. Tin must be pumped at a rate of 4 ml/hr

Functional requirements translated to thermal requirements:

1. Tin in the working volume must be able to reach a temperature of 239°C (250°C with added engineering margins). Additionally, solid tin must be at a temperature of 200°C (due to engineering margins)
2. The speed of melt front of tin must be $\approx$0.68 mm/min (for the working volume designed by [1]) in order to pump tin at the rate of 4 ml/hr (refer appendix A).

2.4. Design Constraints

There are several mechanical, material, and thermal constraints on the operation of the pump. In this work, focus is laid on the thermal constraints. Thermal actuation of the pump requires precise control over the heat flow in the system, and the external factors that lead to challenges in temperature control are listed below.

Thermal Constraints

1. Practical reasons limit the number of heaters that can be used in the system, and the location of the heaters are discrete. However, the tin in the working volume is continuous, and it is challenging to define a continuous temperature control function in order to achieve uniform melting and flow of tin. Non-uniform melting of tin results in entrapment of liquid tin in the working volume (figure 2.3), leading to unpredictable, erratic flow. The possibility of melting tin in a uniform fashion using discretely located heaters is studied using an analytical model in chapter 4.

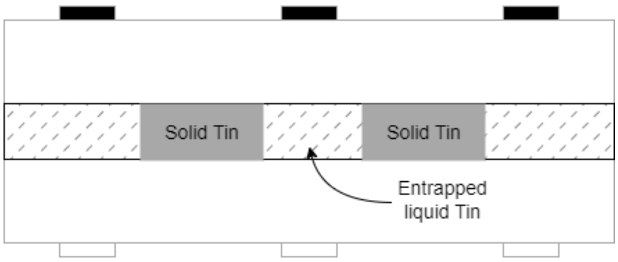

Figure 2.3: Liquid Tin Entrapment

2. Again, due to the discrete location of heaters, the precision of control of temperatures over the length of the working volume is poor. To ensure a good basic control, it must be possible to have solid (200°C) and liquid (250°C) tin in the regions below adjacent heaters in the steady state. The temperature distribution in the pump greatly depends on its geometry, and powers of the heat source and sink. In order to create a steady state thermal gradient of 50 K between solid and liquid tin in adjacent regions, the design needs to be optimized. This is discussed in chapter 5.

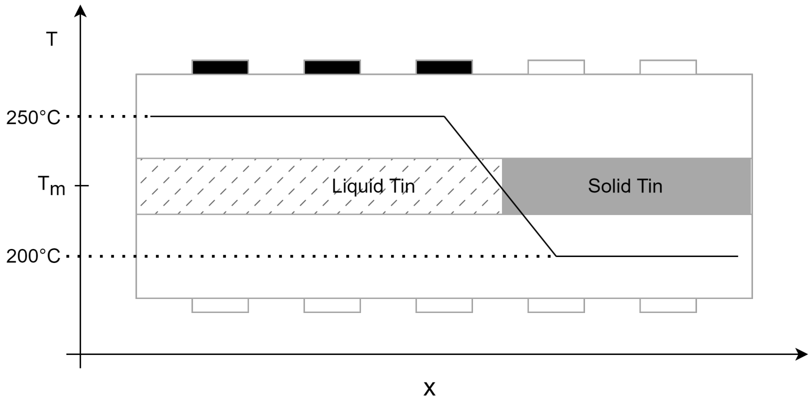

Figure 2.4: Steady state thermal gradient

3. For the operation of the pump, control of tin temperatures is necessary. However, a direct measurement of the tin temperature inside the working volume is not possible. Instead, thermocouples in the system measure temperatures at a location far from tin (figure 2.5), and analytical estimations of tin temperatures have to be made. Accurate estimates of tin temperatures are thus essential. However, tin temperatures are bound to change locally due to non-linear material properties and effects like phase change and pressure build-up, making it hard to predict. The effect of non-linear material properties on tin temperatures is studied and quantified in chapter 6.

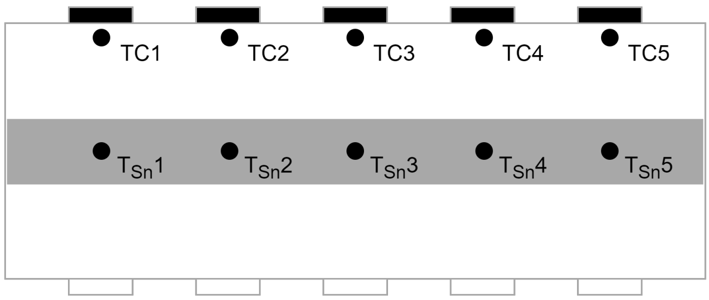

Figure 2.5: Location of thermocouples (TC) in the system. Targeted location of estimation of tin temperatures are marked as T_{Sn})

3

Design of the pump

3.1. Choice of material

The pump body must be made of a material which is a good thermal conductor and also resistant to chemical attack by liquid tin. Refractory metals like W, Mo, Ta meet these requirements (refer table 3.1). Steel, although it has a poor thermal conductivity, is chosen for rapid prototyping of the pump since it is comparatively inexpensive.

3.2. Layout

A basic layout of the pump is shown in figure 3.1. According to flow and volume calculations, the required working volume for the pump and the corresponding thickness of the steel body are worked out in [1] and will not be discussed here. The minimum thickness of the pump body required to withstand pressures generated in the working volume is called the 'safe radius'. The safe radius defines an exclusion zone around the working volume where other components or accessories of the pump shall not be placed. The heaters and sinks are placed outside this exclusion zone. For the ease of understanding and studying the system, the whole geometry is virtually divided into zones, with each zone enclosing a heat source and a heat sink.

	Thermal conductivity (W/m·K)	Thermal diffusivity (mm^2/s)
Tungsten	175 [3]	70 [4]
Molybdenum	138 [5]	50 [6]
Tantalum	57 [7]	24.2 [7]
AISI 316L	16.5 [8]	3.5 [9]

Table 3.1: Thermal properties of some elements

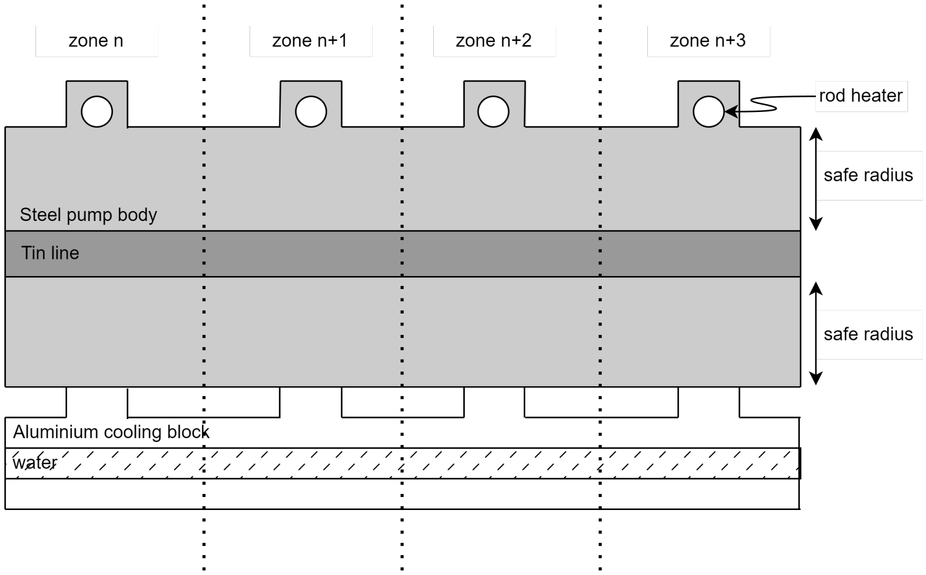

Figure 3.1: A basic layout of the pump

Commercially available rod heaters with an output power of 100W are used as the source of heat. A water-cooled aluminium block is used as the heat sink, which is attached to the pump body in each zone. The contact area between the body and the aluminium block determines the cooling power of the sink.

The heat extracted by the sink is then given by:

$$Q = -h.A.dT \tag{3.1}$$

where h is the heat transfer coefficient between steel and the sink, which has an empirical value of 100 W/(m^2·K) A is the contact area dT is the difference in temperature of steel and the sink at the contact.

3.3. Design parameters

Various design parameters impact the heat flow in the pump:

1. Thickness of the pump body
   - A minimal thickness of the pump body is desirable for rapid temperature changes in the working volume. However, the thickness can be only as small as the safe radius.
2. Cross section of the pump body
   - For a good control over the temperatures, the heat flux from heaters should ideally be orthogonal to the working volume. However, this is practically impossible to achieve since steel is an isotropic thermal conductor. In order to restrict lateral heat flow across zones, the cross section radius of the pump is reduced to a minimum possible value (the safe radius). Refer figure 3.2.
3. Zone length
   - The length of each zone indicates the distance between two heaters. If the heaters are placed too close to each other, the heater in one zone influences the temperatures of the adjacent zone, affecting the steady state thermal gradient between the zones. If heaters are placed too far from each other, the gradient between the center of the zone and the zone edges becomes too high, leading to non-uniform melting and liquid tin entrapment (figure 2.3).
   - The zone length should be such that it is possible to achieve a steady state thermal gradient of 50 K between adjacent zones (figure 2.4).
4. Powers of heat source and sink

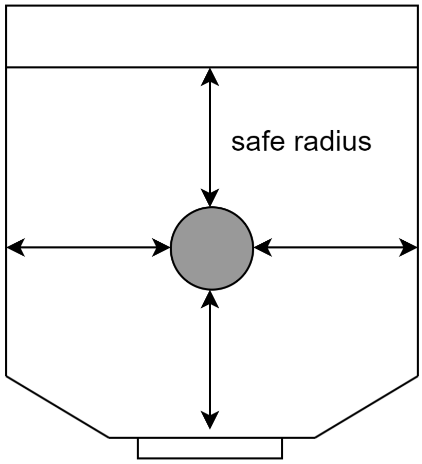

Figure 3.2: Cross section of the pump

- The powers of heat source and heat sink determine the temperatures achieved at the working volume. Practical limitations set the maximum heat input per heater to 100W.
- The amount of heat extracted at the sink can be adjusted by varying the contact area per zone. Higher the contact area, higher the amount of heat extracted (equation 3.1). For an input power of 100W in a zone, the contact area must be optimized such that the working volume can reach temperatures up to 250°C in the steady state.

5. Rate of heat input
    - During simultaneous operation of the heaters in adjacent zones, a very high rate of heat input may produce large thermal gradients between zones leading to liquid tin entrapment. To avoid this, the ramp rates must be limited such that the maximum gradient in the transient state of the pump is 0.5K (1% of the steady state gradient of 50 K).

4
Calculation of ramp rates

Consider a section of the pump with two zones as shown in figure 4.1. In the transient state, we want the heat to be conducted from the center of the zone to the edges as fast as possible. In other words, we want the tin to be heated uniformly along the length without creating a thermal gradient greater than 0.5 K (section 3.3). This is necessary to avoid liquid tin entrapment.

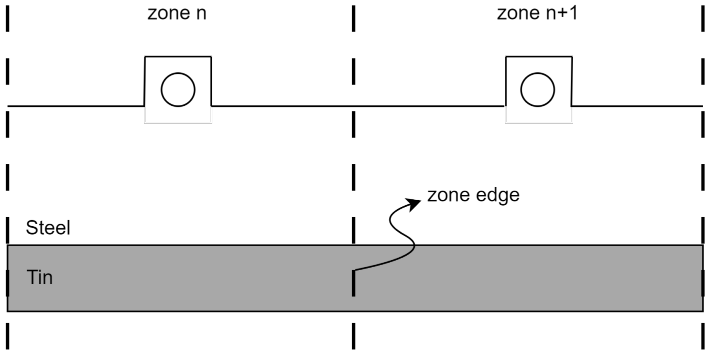

Figure 4.1: Section of the pump

The transient thermal gradient in the section during the heat transfer depends on a number of factors including the zone length, the rate of heat input and also the material properties. By calculating the transient thermal gradients in tin using an analytical model, comments about allowable ramp rates are made.

4.1. Analytical model

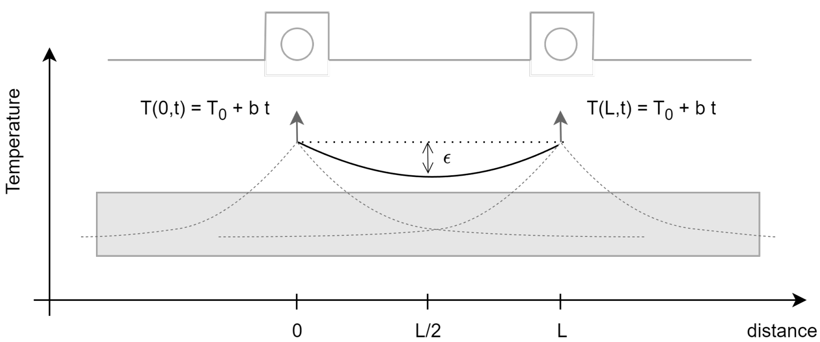

Figure 4.2: Thermal profile in the working volume of the pump, when a constant ramping rate (b) is applied to adjacent zones

Let the working volume be at a uniform initial temperature T_0. The region of interest is the region between the two heaters, $x = [0, L]$. Heat from the heaters ramp the temperature of the planes ($x = 0$ and $x = L$) at a rate of b (K/s). Heat flowing from the point $x = 0$ to the right is approximated to be heat flow in a semi-infinite solid. The same approximation is made for heat flowing from $x = L$ to the left. Hence the region of interest is two superimposed semi-infinite solids with ramped temperatures at the boundaries.

The boundary conditions are thus:

$$T(0, t) = T_0 + b \cdot t \tag{4.1}$$

$$T(L, t) = T_0 + b \cdot t \tag{4.2}$$

Due to the time taken in heat transfer, the time-dependent temperature distribution of tin between the zones will have a curved profile. The transient thermal gradient (ϵ) is measured as the difference between the temperature at the boundary and at the center of the tin line. As discussed in section 3.3, the value of ϵ must be less than 0.5 K.

$$\epsilon = T(0, t) - T(L/2, t) \tag{4.3}$$

For a semi-infinite solid, mathematical expression to calculate the position- and time-dependent temperature (equation 4.5) is known and derived from the conduction equation (equation4.4).

General conduction equation:

$$\frac{\partial T}{\partial t} = \alpha\left(\frac{\partial^2 T}{\partial x^2} + \frac{\partial^2 T}{\partial y^2} + \frac{\partial^2 T}{\partial z^2}\right) \tag{4.4}$$

where α is the thermal diffusivity of the material. Thermal diffusivity, $\alpha = \dfrac{\kappa}{\rho \cdot C_p}$ m^2/s, where κ is the thermal conductivity, ρ is the density, and C_p is the adiabatic heat capacity.

Governing equation [10] (solution of conduction equation):

$$\frac{T(x,t) - T_0}{bt} = \left(1 + \frac{x^2}{2\alpha t}\right)\left(1 - erf\left(\frac{x}{2\sqrt{\alpha t}}\right)\right) - \frac{x}{\sqrt{\pi}\sqrt{\alpha t}} exp\left(\frac{-x^2}{4\alpha t}\right) \tag{4.5}$$

In our case, the temperature profile of tin due to the left boundary is given by equation 4.5. The temperatures due to the right boundary can be derived with a slight modification:

$$\frac{T(x,t) - T_0}{bt} = \left(1 + \frac{(L-x)^2}{2\alpha t}\right)\left(1 - erf\left(\frac{(L-x)}{2\sqrt{\alpha t}}\right)\right) - \frac{(L-x)}{\sqrt{\pi}\sqrt{\alpha t}} exp\left(\frac{-(L-x)^2}{4\alpha t}\right) \tag{4.6}$$

The superimposed temperature distribution in tin is then given by the sum of equations 4.5 and 4.6. Temperature at $x = L/2$ at time t is then

$$\frac{T(L/2,t) - T_0}{bt} = 2 * \left(1 + \frac{(L/2)^2}{2\alpha t}\right)\left(1 - erf\left(\frac{(L/2)}{2\sqrt{\alpha t}}\right)\right) - 2 * \frac{(L/2)}{\sqrt{\pi}\sqrt{\alpha t}} exp\left(\frac{-(L/2)^2}{4\alpha t}\right) \tag{4.7}$$

Using the definition of ϵ (equation 4.3),

$$\frac{\epsilon}{bt} = 1 - 2 * \left(1 + \frac{(L/2)^2}{2\alpha t}\right)\left(1 - erf\left(\frac{(L/2)}{2\sqrt{\alpha t}}\right)\right) + 2 * \frac{(L/2)}{\sqrt{\pi}\sqrt{\alpha t}} exp\left(\frac{-(L/2)^2}{4\alpha t}\right) \tag{4.8}$$

From this expression, it can be seen that the gradient (ϵ) depends on the zone length (L), ramping rate of boundary temperature (b), diffusivity of tin (α), and also time (t). Thermal diffusivity of tin is taken to be $\alpha = 40$ mm^2/s [11].

In diffusion problems, it is convenient to measure time as multiples of the characteristic diffusion time, τ. The characteristic diffusion time is defined as: $\tau = \dfrac{L^2}{\alpha}$, where L is the length of the system over which diffusion happens and α is the thermal diffusivity. Per definition, τ is the time taken for the system to reach 63.2% of its final steady state. At a duration of five times the characteristic diffusion time (5τ), the system reaches 99% of its steady state, and is considered as sufficient time to reach equilibrium. Hence, melting is considered to be uniform if the transient thermal gradient ϵ is lower than 0.5 K after a time of 5τ.

4.2. Results

For a length of L = 5 mm, the transient gradient (ϵ) for different ramp rates (b) is plotted in the figure 4.3. The calculated gradient for different ramp rates is plotted at five instances, which are multiples of the characteristic diffusion time.

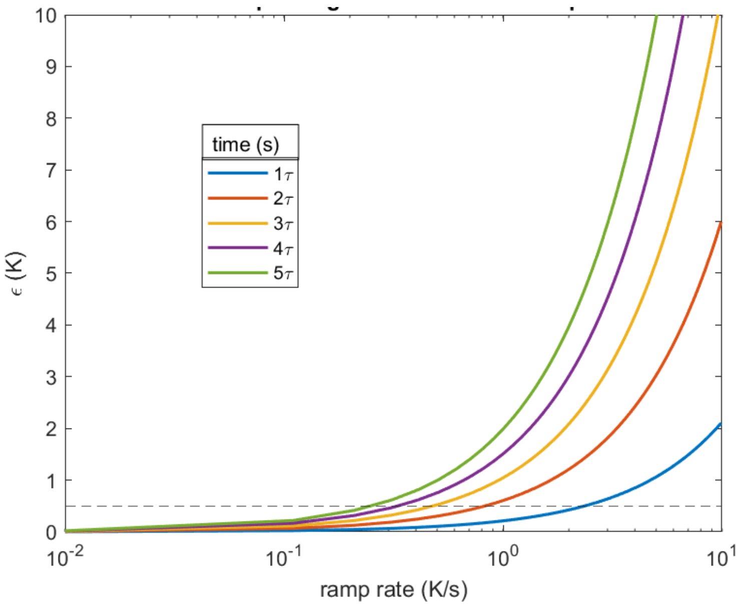

Figure 4.3: Transient thermal gradient ϵ with passing time for different ramp rates at the boundaries. L =5 mm

The characteristic diffusion time in our model, $\tau = \dfrac{L^2}{\alpha} = \dfrac{5^2}{40} = 0.6s$.

From figure 4.3, it can be seen that uniform heating (ϵ < 0.5 for time = 5τ) over the length L is possible when the ramp rates are of the order of 0.1 K/s or lower.

Consider that this ramp rate is applied to melt solid tin over the length L. A temperature rise of 50 K is needed to melt solid tin (200°C) to liquid (250°C) (section 2.3). The time taken for the phase transformation is then:

$$t_{melting} = \frac{L}{b} = \frac{50}{0.1} = 500 \text{ s.}$$

In terms of speed of the melt front, this translates to:

$$\text{speed of melt front} = \frac{L}{t_{melting}} = \frac{5}{500} = 0.01 \text{ mm/s} = 0.6 \text{ mm/min.}$$

This speed is of the order of the required speed of the melt front for the pump (refer section 2.3).

4.3. Discussion

The results of this analysis show that it is possible to melt tin in the working volume uniformly over a given length, provided that the ramp rates are of the order of 0.1 K/s, for a zone length of 5 mm. However, for higher values of length L, the characteristic diffusion time is higher, and even lower ramp rates are required to keep the transient gradient below 0.5 K. This results in lower speeds for the melt front than required for a pumping capacity of 4 ml/hr.

It has to be noted that in this analytical model, it is assumed that the heaters only ramp the plane in which they are located, at the rate of b K/s (figure 4.2). However, in practice, heat from the heaters is conducted directly over the entire length of the working volume. This enhances temperature homogeneity along the length of the section, potentially allowing for faster ramp rates, shorter heating durations, and faster melt front speeds. This can be investigated with a more representative model of heat flow in the system.

The time taken for heat diffusion through the pump body depends on the thermal diffusivity of the material. Materials with a higher thermal diffusivity have lower diffusion times, which allows for higher speeds of the melt front. The possible ramp rates and speeds of melt front for materials with higher thermal diffusivity (table 3.1) than steel need to be investigated.

The rate of heat extraction by the sink also impacts the temperature distribution in tin, just like the rate of heat input from the heaters. Adjusting both heating and cooling powers simultaneously may offer better control over tin temperatures. This possibility as well can be investigated with a more representative model of heat flow in the system.

5 Optimization of pump geometry

In order to be able to reach a steady state gradient of 50 K in the adjacent zones in the working volume, the free design variables - zone length and sink contact area (3.3) must be optimized. This is done by simulating and evaluating the thermal response of the pump using finite element analysis (Ansys Workbench). Numerical modeling allows for a quick investigation of the thermal profiles of various geometries of the pump, which is very helpful for optimization. The greatest advantage of modeling is that it makes it possible to study the temperatures at locations inside the pump which cannot be physically measured.

5.1. Geometry

The geometry of the pump in the numerical model is shown in figure 5.1. Zone length is L and the sink contact area is A. The temperature of tin (T_{Sn}) is measured at the center of the working volume in each zone.

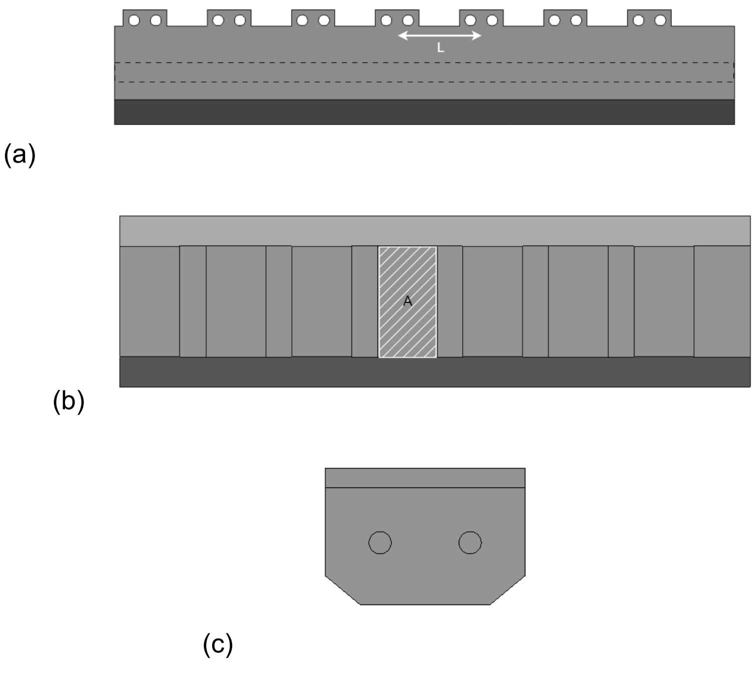

Figure 5.1: (a) Lateral view of the pump; zone length is highlighted as L. (b) bottom view of the pump; contact area with sink is highlighted as A. (c) Cross section of the pump showing two adjacent channels for tin as the working volume

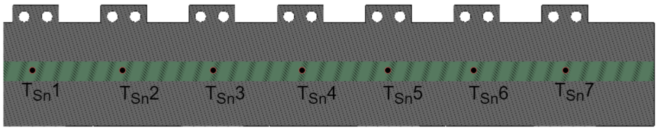

Figure 5.2: Lateral section of the pump showing locations of Tin temperature measurement

5.2. Material Properties

The material properties essential for thermal analyses include thermal conductivity, heat capacity, density, melting point, and latent heat of fusion. These properties tend to vary with varying temperatures and pressures. For the sake of simplicity, material properties at 232°C are chosen and are assumed to be constant. This is also good enough since the goal of this exercise is to optimize the pump geometry around the operating temperature (232°C). The heat transfer coefficient of water at the sink is 100 W/(m^2·K) at 22°C.

The material properties of steel and tin used in this thermal analysis are listed in table 5.1:

	units	AISI 316L	Tin
Thermal conductivity	W/m·K	16.5 [8]	66 [12]
Specific heat capacity	J/g-K	0.5 [9]	0.21 [13]
Density	g/cm^3	7.89 [9]	7.26 [14]

Table 5.1: Physical properties of AISI 316L and Tin

5.3. Boundary conditions

The boundary conditions are heat input from the heaters and convective heat transfer at the sink. Input power of 100 W is applied at the surface where rod heaters contact the pump body. The equivalent of sink is a convective boundary condition at the contact area, with a heat transfer coefficient of 100 W/(m^2·K).

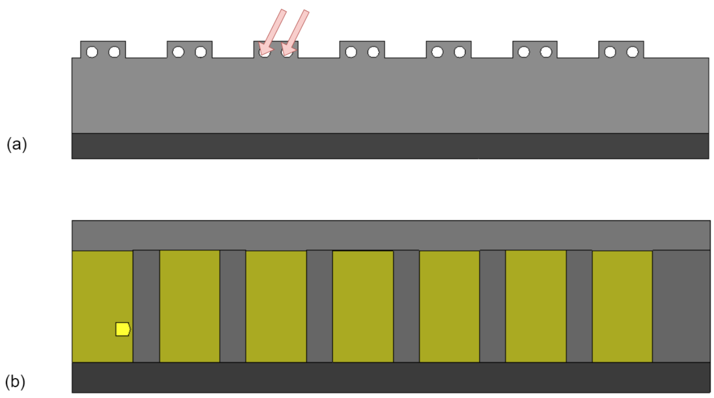

Figure 5.3: Boundary conditions of the model. (a) heat input from heaters is highlighted in red arrows (b) heat extraction by sink is highlighted in yellow

Heater ON	Gain (K/W)							
	TSn1	TSn2	TSn3	TSn4	TSn5	TSn6	TSn7	TSn8
H1	1.19	0.74	0.4	0.22	0.12	0.07	0.04	0.03
H2	0.75	1	0.63	0.34	0.19	0.11	0.06	0.04
H3	0.41	0.63	0.94	0.6	0.32	0.18	0.11	0.07
H4	0.22	0.34	0.6	0.91	0.59	0.32	0.19	0.13
H5	0.13	0.19	0.32	0.59	0.92	0.6	0.34	0.22
H6	0.07	0.11	0.18	0.32	0.6	0.93	0.63	0.41
H7	0.04	0.06	0.11	0.19	0.34	0.63	1.01	0.75
H8	0.03	0.04	0.07	0.12	0.22	0.4	0.74	1.19

Figure 5.4: An example gain matrix (G)

5.4. Evaluation of results

The model is solved for the applied boundary conditions to retrieve the steady state temperature distribution. Two parameters are defined to evaluate the thermal response of various geometries - Gain matrix and Crosstalk.

5.4.1. Gain Matrix

The rise in temperature of Tin for the given input power is defined as gain. Numerically,

$$\text{gain} = \frac{\text{rise in tin temperature in zone 'n'}}{\text{power input of heater in zone 'n'}} = \frac{\mathrm{d}T_{Sn}}{\mathrm{d}P}(K/W)$$

The gains obtained at each zone as an effect of the heat from each heater are captured in a matrix called the gain matrix. The rows of the matrix represent the heater in operation, and the columns represent the respective gains in each zone. An example gain matrix for a system with eight zones is shown in figure 5.4. It can be seen that the gain values are the least at the center and the highest at the ends. This is because for a zone at the center, the number of sink contacts present in the vicinity are double the number of contacts for the zones at the edges.

5.4.2. Crosstalk

The phenomenon where a signal or impulse creates a response at any location other than the designated location is called crosstalk. In the pump, the heat from one zone heating up the adjacent zones is considered to be crosstalk. The crosstalk in the pump is numerically defined as the contrast between gains of the adjacent zones. When the contrast is low, it shows that the heat spread across zones is high, and vice versa.

$$\text{crosstalk} = 1 - \text{observed contrast between gains of adjacent zones} \tag{5.1}$$

Crosstalk is measured at the center of the pump where it is the highest, since the extent of heat spread is maximum. For the gain matrix in fig.5.4 the crosstalk between zones 4 and 5 when Heater 4 is ON, is calculate as $1-(0.91-0.59) = 0.68$.

5.4.3. Inverse Gain matrix

The gain matrix shows the rise in temperature per unit power input. The product of the gain matrix (G) and the array of heater powers gives an array of tin temperatures (T_{Sn}) in the zones.

$$[T_{Sn}] = G \times [P]$$

where $[T_{Sn}]$ is the vector of tin temperature in the zones and $[P]$ is the vector of input power from heaters across the zones. Then the inverse gain matrix should give the required input power to bring about a certain difference in temperature.

$$[P] = G^{-1} \times [T_{Sn}]$$

This is a powerful way to evaluate whether it is possible to achieve a gradient of 50K between adjacent zones in the respective configuration.

For example, let the matrix in figure 5.4 be the gain matrix (G) of the pump for chosen values of A and L. To achieve the following target tin temperatures in this configuration,

$$[T_{Sn}] = \begin{bmatrix} 200 \\ 200 \\ 200 \\ 200 \\ 250 \\ 250 \\ 250 \\ 250 \end{bmatrix}$$

the required input powers of the heaters are:

$$[P] = G^{-1} \times [T_{Sn}] = \begin{bmatrix} 94.87 \\ 45.11 \\ 71.45 \\ -7.95 \\ 137.237 \\ 62.79 \\ 62.00 \\ 117.73 \end{bmatrix}$$

The negative heater power in zone 4 indicates that either:

1. the heat flux out of the sink in that zone is insufficient to bring down the temperatures to 200°C (low sink area), or
2. the heat spread from the adjacent zone into this zone is very high (high crosstalk).

This makes it not possible to achieve a gradient of 50K with the chosen combination of parameters (L and A). This means that this combination will not result in a functional design.

5.5. Results of parameter Study

The thermal profiles for different combinations of parameters are analysed in order to find the optimal combination. To start with, an arbitrary choice of zone length of 50 mm and sink contact area of 45$\times$25 mm^2 is analysed, and the parameters are iteratively updated based on the findings. Using three zone lengths (50 mm, 100 mm, 140 mm) and three sink contact areas (45$\times$25 mm^2, 65$\times$35 mm^2, 65$\times$40 mm^2) (refer figure5.5), nine combinations of the free parameters are analysed in total.

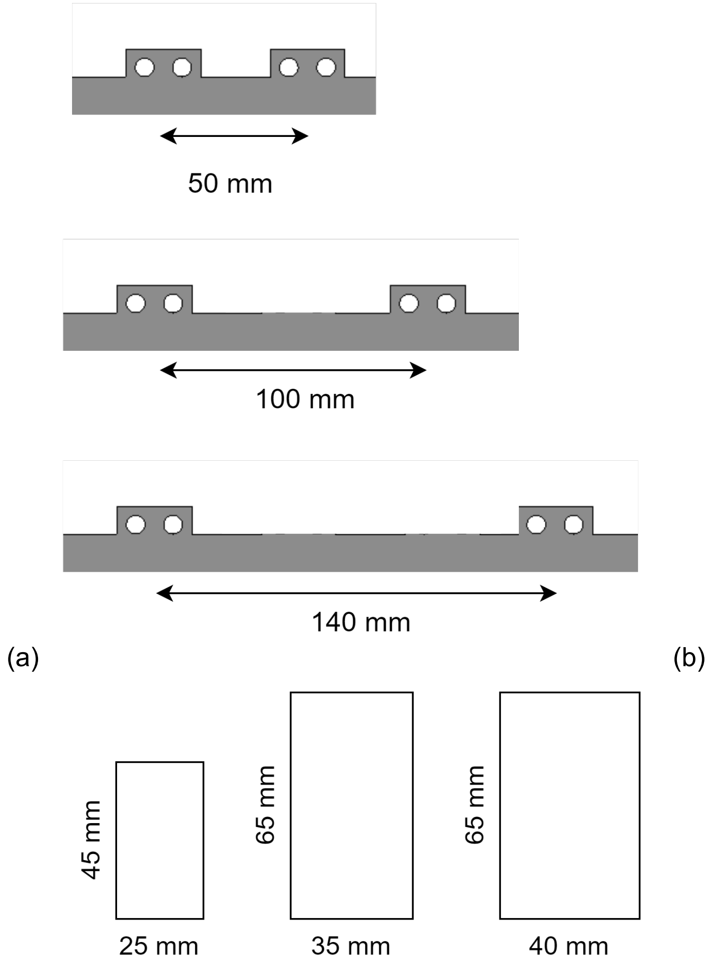

Figure 5.5: (a) different zone lengths and (b) different sink contact areas used in the parameter study

As an example, the steady state temperature distribution in the pump for a zone length of 50 mm and sink area of 65×35 mm^2 is shown in figure 5.6. Heater number 3 is at a power of 100 W, and the effective heat transfer coefficient at the sink is 100 W/(m^2·K).

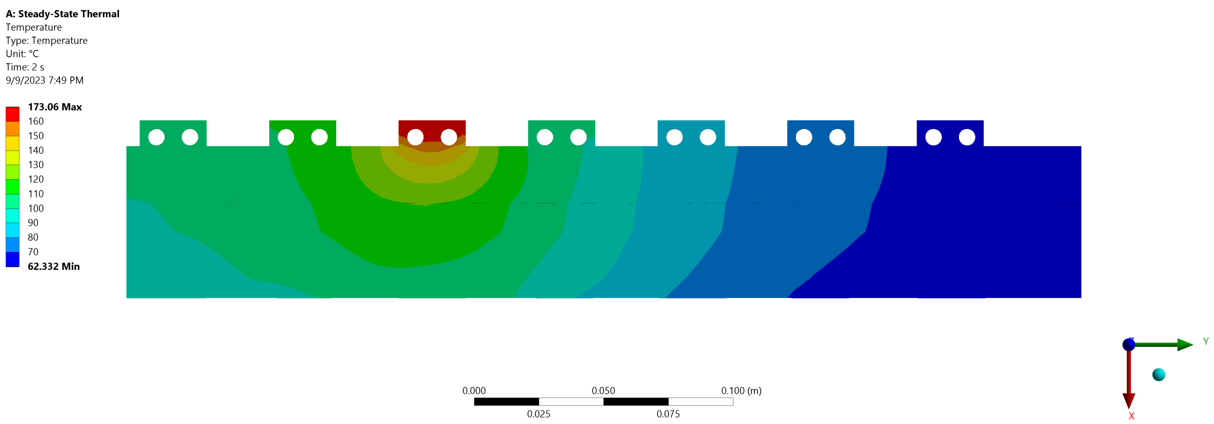

Figure 5.6: Steady state temperature profile of the pump with a zone length of 50mm and sink area of 65×35mm^2

The results of the parameter study are summarized in tables 5.2 and 5.3.

Zone length (mm)		Sink contact area (mm x mm)		
		45 x 25	65 x 35	65 x 40
	50	1.52	1.09	0.55
	100	1.31	0.99	0.95
	140	1.21	0.99	0.79

Table 5.2: Values of gain for some chosen values of zone length, and area of contact with sink (Higher is better)

Zone length (mm)		Sink contact area (mm x mm)		
		45 x 25	65 x 35	65 x 40
	50	0.63	0.65	0.71
	100	0.55	0.58	0.58
	140	0.48	0.51	0.47

Table 5.3: Values of crosstalk for some chosen values of zone length, and area of contact with sink (Lower is better)

5.6. Discussion

- An increase in contact area significantly reduces gain. For a zone length of 50 mm, when the contact area doubles, gain reduces by 28%. Also for zone lengths of 100 and 140 mm, gain reduces by 24% and 21% respectively.
- An increase in contact area does not significantly affect crosstalk between the zones. For a zone length of 50 mm, crosstalk slightly increases with increasing contact area, but a similar trend is not observed for other zone lengths. Hence there is poor correlation between sink contact area and crosstalk
- An increase in zone length reduces gain. For a sink contact area of 45×25 mm^2, when the zone length doubles, gain reduces by 14%, and when zone length triples, gain reduces by 20%. The impact of zone length on the gain values is not as significant as the effect of contact area.
- An increase in zone length slightly reduces crosstalk. For a sink contact area of 45×25 mm^2, when the zone length doubles, crosstalk reduces by 13%, and when zone length triples, crosstalk reduces by 24%. Similar trend is observed for other contact areas. Hence the impact of zone length on crosstalk is more significant compared to the impact of sink contact area.

The overall effect of the parameters on temperature gain and crosstalk between zones is summarized in table 5.4.

zone length		Sink contact area	
		low	high
	low	high gain high crosstalk	low gain high crosstalk
	high	high gain low crosstalk	low gain low crosstalk

Table 5.4: Summary of the effect of design parameters

It can be seen that there are opposing requirements of parameters for our two objectives (maximize gain, minimize crosstalk). Calculations using the inverse gain matrix (Appendix C) shows that it is possible to achieve a steady state thermal gradient of 50 K when the zone length is 140 mm. And for a zone length of 140 mm, maximum gain is reached when the sink contact area is 45×25 mm^2. Hence, an optimal combination of parameters is found in the middle-ground (low contact area of sink, and a high zone width), and has a slight trade-off of gain and crosstalk.

It has to be noted that this geometry is optimized such that tin can reach temperatures of 200°C and 250°C, and a gradient of 50 K can be created between adjacent zones in the steady state. The transient state of the pump, such as, the time taken to reach these temperatures is not taken into account. For example, a zone length larger than 140 mm can further decrease crosstalk, but the time taken to heat/cool the tin at the far end of the zones will increase. Likewise, a sink contact area smaller than 45×25 mm^2 can give even higher gains, but the time taken to freeze the tin will increase.

The current geometry is optimized such that tin can undergo phase changes, provided sufficient time is allowed to reach the steady state. Hence, it is useful to validate the pressure build-up capacity of the pump. The geometry can further be optimized by also taking its transient state into account, which will be useful in validating the pumping capacity.

6

Impact of non-linear properties on temperature distribution

In order to quantify the impact of non-linear properties of tin on temperature distribution in the working volume, a finite difference model is built in MATLAB. The model includes enthalpy-temperature curves of tin and steel to estimate the temperature distribution in the system.

6.1. The Finite Difference Model

6.1.1. Geometry

Consider a lateral section of one zone of the pump, as shown in figure 6.1. The length of the section is as optimized in chapter 5 (zone length), and the thickness of the section into the plane of the paper is chosen arbitrarily. The location of measurement of the control temperature (TC) and the location of estimation of tin temperatures (T_{Sn}) are shown.

6.1.2. Boundary conditions

The pump body and the sink are at a uniform initial temperature (T_0) of 22°C. The locations of heat source and heat sink are shown in figure 6.1 (b). Since the focus is to study the local temperature distribution in tin, the power of heat source is arbitrarily chosen such that tin can reach sufficient temperatures to undergo phase changes.

6.1.3. Material Properties

The properties of steel and tin used in this model are same as those used for FEM simulations (refer 5.1). In addition, the enthalpy-temperature curves of the metals are used to convert the calculated enthalpies of the elements into temperatures or vice-versa. Enthalpy of a system is not a definite property, but is the internal energy of the system at the given temperature. The change in enthalpy of the system with temperature is definite, and can be calculated using $dH = \rho \cdot Cp \cdot dT$.

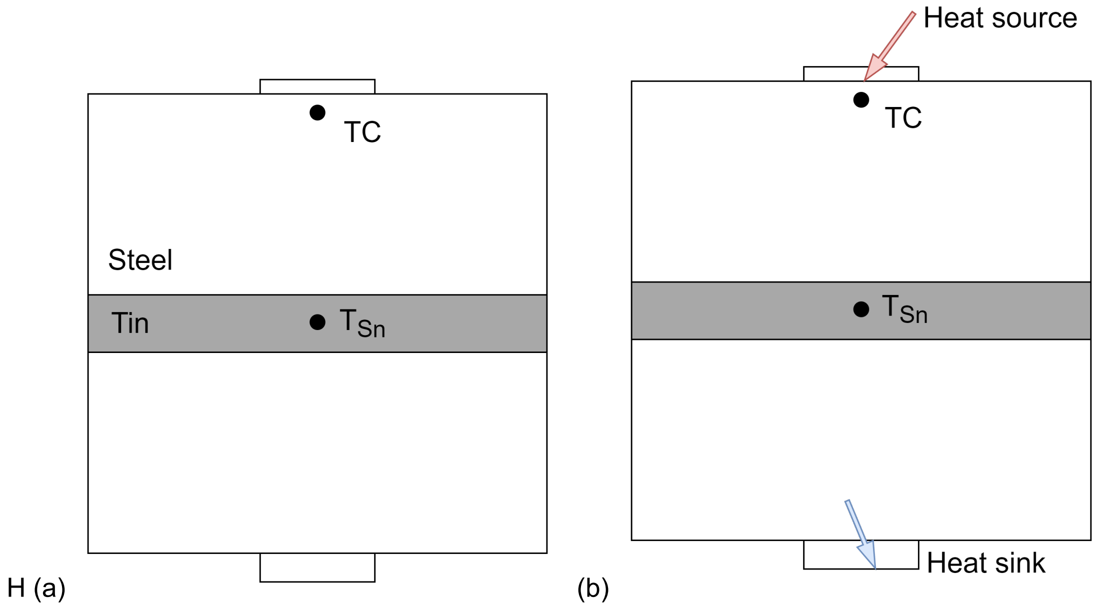

Figure 6.1: (a) One zone of the pump as the geometry for the Finite Difference Model (b) Location of heat source and heat sink

	units	AISI 316L	Tin
Specific heat capacity	J/g-K	0.5 [8]	0.28 (solid) 0.21 (liquid)
Latent heat of fusion	J/m^3	-	4.37×10^8

Table 6.1: Thermal properties of AISI 316L and tin

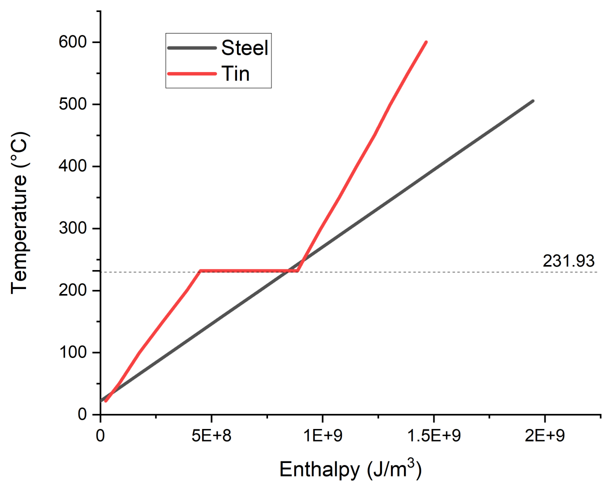

Figure 6.2: The temperature-enthalpy curves of Steel and Tin [13, 15]

The values of specific heat of steel, tin, and the enthalpy of fusion of tin, as taken from the graphs, are given in table 6.1.

6.1.4. Meshing

This simple slab-like geometry is discretized with a hexahedral mesh. The elements are given an aspect ratio close to 1 in order to ensure a good accuracy of the simulation [16]. The thickness of the section in the third dimension (into the plane of the paper) is of the order of the element size. The elements are indexed with consecutive numbers starting with 1.

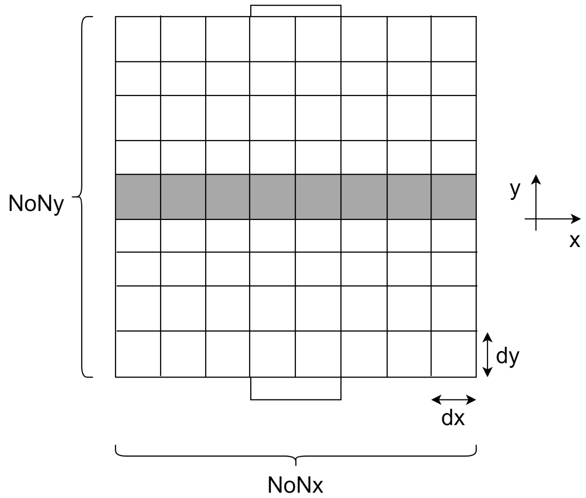

Figure 6.3: The model geometry discretized into a number of elements

For a finite difference model such as this, the choice of mesh resolution, step size, number of iterations, and the convergence tolerance are interdependent, and are chosen by trial-and-error to make the simulation converge.

6.1.5. Conductance matrix

In this thermal model, heat flow between elements causes temperature changes and temperature difference between elements causes heat flow. It is essential to define the interactions between the elements for this simulation, which is thermal conductance.

Consider an element in the mesh indexed 'n' as shown in figure 6.4. Element n has four adjacent elements at four faces, which are indexed $n+1, n-1, n-NoNx, n+NoNx$ in $+x, -x, +y, -y$ directions, respectively. Elements n and $n+1$ are both made of steel. The heat flow between these elements is:

$$Q = -\kappa_{steel} \cdot A \cdot dT/dx$$

where κ_{steel} is the thermal conductivity of steel, $A = (dy \times dz)$ is the area of contact between the elements, and dx is the distance between the elements.

The thermal conductance between elements n and $n+1$ is:

$$K_{n,n+1} = \kappa_{steel} \cdot A/dx = \kappa_{steel} \cdot \frac{(dz \times dy)}{dx}$$

Element $n + NoNx$, on the other hand, is made of tin, and the conductance between them (thermal resistance adds up in series) is given by:

$$\frac{1}{K_{n,n+NoNx}} = \frac{0.5 \times dy}{\kappa_{steel} \cdot (dx \times dz)} + \frac{0.5 \times dy_{tin}}{\kappa_{tin} \cdot (dx \times dz)}$$

The interaction between an element in the steel body in contact with sink is half conduction and half convection. Hence the conductance between a steel element and the sink is defined as:

$$K_{steel,sink} = \kappa_{steel} \cdot \frac{(dx \times dz)}{0.5 \times dy} + h \cdot (dx \times dz)$$

where h = 100 W/(m^2·K) is the heat transfer coefficient at the sink.

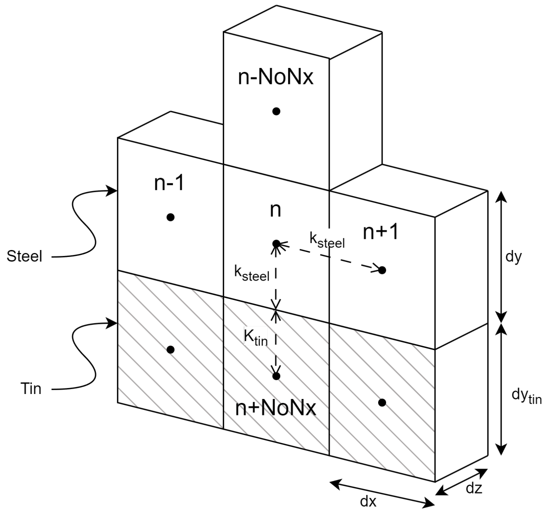

Figure 6.4: A segment of the mesh showing conductance between nodes

In such a way, the conductance between all pairs of interacting elements in the mesh are captured in a conductance matrix. The conductance matrix $[K]$ is a square matrix whose order is equal to the number of elements in the mesh. If $[T]$ is an array of temperatures of all elements in the model, then a conductance matrix $[K]$ is defined such that their product gives an array $[Q]$ of the heat flowing in or out of the elements: $[Q] = [K] \times [T]$

6.2. Computing the Steady State temperature distribution

The initial temperatures of the elements $[T_0]$ are known, and the initial enthalpies $[H_0]$ are calculated from $[T_0]$ using the temperature-enthalpy curves 6.2 as:

$$H_0 = H_{T_0} \times (dx \times dy \times dz)$$

The enthalpy of an element, and hence its temperature, changes due to the heat flowing in from the heaters, or heat lost to the sink, or the heat exchange between elements due to difference in temperatures. To calculate the steady state temperature distribution, the temperatures of the elements are repeatedly updated in infinitesimally small steps using the following four steps:

1. Heat flow between elements is driven by thermal gradients between an element and its neighbours. The amount of heat flowing in or out of an element is calculated using the conductance matrix as

$$[Q] = [K] \times [T]$$

2. To this array, the heat from the heaters, $Qext$, is added to the elements in contact with the heat source. The net change in heat of an element is thus

$$[\Delta Q] = [Q] + Q_{ext}$$

3. Enthalpy of the elements are updated by adding the change in heat ΔQ. Heat and enthalpy are related as:

$$\Delta H = \Delta Q + P\Delta V + V\Delta P$$

where $P\Delta V = \Delta H_{expansion}$ is the change in enthalpy due to change in volume, and $V\Delta P = \Delta H_{pressure}$ is the change in enthalpy due to change in pressure.

$V\Delta P$: Under nominal operation, the pressure built in tin also acts on the solid tin in the working volume, so the change in enthalpy due to pressure ($H_{pressure}$) is the same for all elements of tin, and is hence ignored.

$$V\Delta P = 0$$

$P\Delta V$: Tin expands by about 2.7% on melting [1]. For a tin volume of Vm^3 and a targeted pressure rise of 1400 bar in the pump, the change in enthalpy is:

$$\Delta H_{expansion} = P\Delta V = 1400(bar) \cdot 0.027 \cdot V(m^3) \tag{6.1}$$
$$= 1400 \times 10^5(Pa) \cdot 0.027 \cdot V(m^3) \tag{6.2}$$
$$= 3.78 \times 10^6 \cdot V(J) \text{ or } 3.78 \times 10^6(J/m^3) \tag{6.3}$$

$\Delta H_{expansion}$ is two orders of magnitude smaller than the latent heat of fusion ($\Delta H_f^{Tin} = 4.37 \times 10^8$ J/m^3), and hence its effect on change in enthalpy is negligible. Thus, $\Delta H = \Delta Q$

4. The enthalpies of the elements are updated by adding the change in enthalpy (ΔH) to the original enthalpies from the previous step.

$$[H]' = [H] + [\Delta H] \tag{6.4}$$
$$[H]' = [H] + [\Delta Q] \tag{6.5}$$
$$[H]' = [H] + [Q] + Q_{ext} \tag{6.6}$$

where $[H]'$ is the array of updated enthalpies of elements.

5. The updated enthalpy ($H + \Delta H$) is then translated into updated temperature ($T + \Delta T$) of the elements using the enthalpy-temperature curve 6.2.
6. The updated temperatures $[T]'$ are then fed back to step 1, and the loop is repeated until the steady state is reached.

6.3. Computing the Transient temperature distribution

In order to record the transient temperature distribution with time, temperatures of the elements ($[T]$) are updated in small step sizes, following the same procedure as in computing the steady state. In addition, the step size of each iteration (dt) is recorded as the actual time interval (in seconds) in which the calculated update in temperature happens.

Consider an arbitrary element in the mesh. The amount of heat added to/extracted from this element decreases with time until the steady state is reached (figure 6.5). Simultaneously, the temperature of this element changes with time until the steady state is reached. The total time taken (in seconds) for Q and T to reach the steady state are the same. Hence a small step dt used to calculate the change in heat/enthalpy of the element is also the actual time interval (in seconds) in which the temperature change (dT) happens.

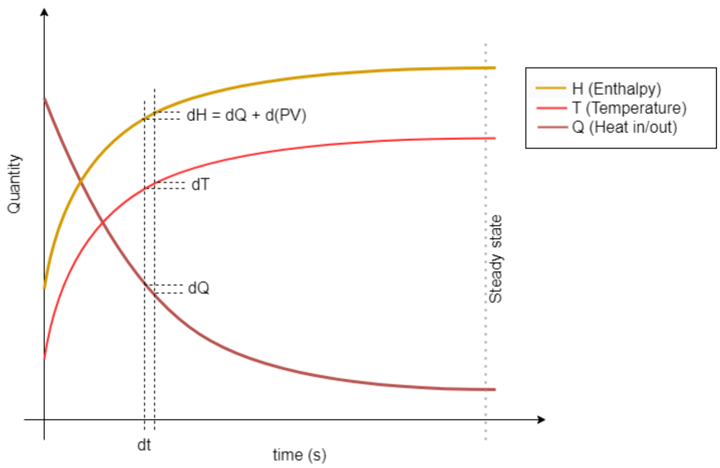

Figure 6.5: Transient state of the temperature, heat and enthalpy of an arbitrary element in the model

6.4. Results & Discussion

The transient temperatures of tin (T_{Sn}), for the cases of linear properties (without considering latent heat during melting) and non-linear properties (with absorption of latent heat during melting) of tin are shown in figure 6.6.

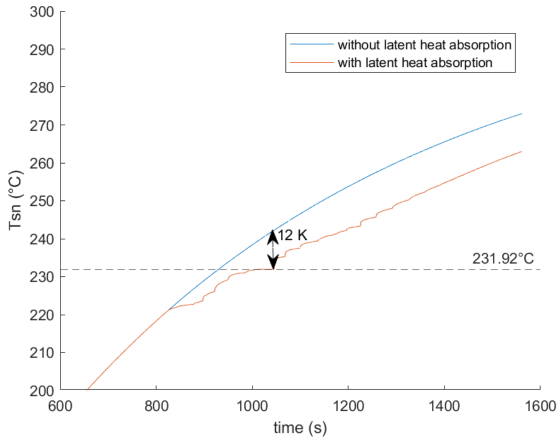

Figure 6.6: Temperature of tin over time, with and without the absorption of latent heat during melting

It can be seen that the absorption of latent heat during melting results in a tin temperature of about 12 K less than what would have been without the absorption of latent heat. Also, with the absorption of latent heat, it takes 115 seconds longer for the location of T_{Sn} to surpass the melting point (231.92°C) compared to no latent heat. The control system in itself is not capable of detecting phase changes or the movement of melt front, and its transfer function must be defined in such a way that it is able to account for this difference/delay while estimating/controlling tin temperatures.

Further, it is also observed that the tin temperature (T_{Sn}) starts to retard even before the melting point is reached. This is because T_{Sn} is measured at the center of the tin volume. The region of tin above the location of T_{Sn} is the closest to the heaters. When this region reaches the melting point and starts melting, the absorption of latent heat prevents the temperature rise of tin in and around it. This is the reason why a retardation is seen in T_{Sn} even before the melting point is reached.

Another non-linear property of Tin is its pressure-dependent melting point. Pressure build-up in the working volume can significantly impact the phase distribution of tin and consequently, the movement of melt front. It is worth investigating how pressure-build up affects the temperature distribution in tin.

7 Conclusions

In this thesis, we addressed three thermal constraints in a phase change tin pump by examining three aspects of temperature distribution in the system:

7.1. Transient thermal gradient

- The heaters in the pump are placed at discrete locations, but the working volume is continuous. The possibility of achieving uniform heating of the working volume using discrete heaters without creating a transient thermal gradient over 0.5 K was investigated using an analytical model.
- For a zone length of 5 mm, it is found that a ramp rate of the order of 0.1 K/s is required to achieve uniform heating.
- This translates to a melt front speed of 0.6 mm/min, which is of the order of the speed required for a pumping capacity of 4 ml/hr.

7.2. Steady state thermal gradient

- Since the number of heaters are limited, a precise control over the temperature of tin at any given location is difficult. The possibility to create adjacent zones of solid and liquid tin in the working volume ensures a good basic control.
- The geometry of the pump has a significant impact on its thermal behavior (section 3.3). Geometry requirements in order to create a steady state thermal gradient of 50 K between adjacent zones in the pump was explored by setting up a parametric study using finite element analysis.
- It is found that the two free parameters (zone length, sink contact area) have contradicting requirements to meet the objectives of maximizing temperature gain and minimizing crosstalk between zones.
- In order to increase gain, zone length and sink contact area must be low. On the other hand, in order to decrease crosstalk, the zone length and sink contact area must be high.
- A combination of high zone length (140 mm) and low sink contact area (45×25 mm^2) was found to be an optimal configuration, with a slight trade-off on both the objectives.

7.3. Non-linear material properties

- A direct measurement of temperature of tin inside the pump is not feasible, so the temperatures are estimated analytically. Accurate estimations of the tin temperatures are essential for pump operation.
- The effect of absorption of latent heat during melting on the local temperature distribution in tin is studied using a finite difference model.
- Absorption of latent heat during melting results in a temperature of 12 K lower than what would be if there were no latent heat.
- Absorption of latent heat effectively delays the movement of melt front of tin by 115 seconds compared to that without the effect of latent heat.
- The control system of the pump must be capable of taking these differences into account when estimating/controlling tin temperatures.

8

Recommendations for future work

8.1. Transient thermal gradient

- In the analytical model used in chapter 4, it was assumed that the heaters only ramp the temperature of the plane they are in, which form the ends of the section. However, in practice, heat from the heaters also reach the entire length of the section to some extent. This improves the uniformity of temperature distribution in tin and increases the possibility of applying higher ramp rates, and over longer zone lengths. This can be investigated using more representative models of the system.
- The uniformity of temperature distribution in tin also depends on the rate of rate of heat extraction by the sink, similar to the rate of heat input by heaters. Adjusting both heating and cooling rates simultaneously with time offers better control over tin temperatures in the transient state. This also means better control over the movement of meltfront, hence this possibility has to be investigated.
- Along with improved control, it is also important to investigate the possibility of achieving a constant speed of melt front. A constant speed of melt front is essential in order to reach a constant flow rate of tin, which his targeted to be at 4 ml/hr.

8.2. Steady state thermal gradient

- The geometry optimization using finite element analysis (chapter 5) does not take into account the transient state of the pump. For practical operating conditions, the time taken to drive the phase changes of tin is important, because it determines the pumping capacity and the speed of operation. For instance, a zone length higher than the optimized value can further reduce crosstalk, but will increase the time taken to melt tin at the far end of the zones. Similarly, a sink contact area lower than the optimized value can further increase gain, but will decrease the time taken to solidify tin due to the lowered cooling rate. Thus, the geometry of the pump needs to be further optimized for its pumping capacity, by taking its transient state into account.

8.3. Non-linear material properties

- In addition to the absorption of latent heat, another non-linear property of tin is its pressure-dependent melting point. The effect of pressure build-up on the temperature distribution in tin needs to be investigated, which helps with more accurate estimations of tin temperatures. In order to do this, the finite difference model discussed in chapter 6 can be extended such that it can compute the pressure build-up in the system as well.
- Further, pressure build-up could significantly impact the phase distribution of tin, due to the pressure-dependency of its melting point. Consequently, this impacts the shape and movement of the melt front, and in turn, the pumping capacity. To this end, the effect of pressurization on the shape and movement of melt front also needs to be studied.

References

[1] Bashir Mazaheri. *Mechanical design of phase change tin pump [unpublished]*. Tech. rep. ASML, 2023.

[2] Jr Stanley E babb. *Melting curve of tin and selenium to 10000 bars*. Tech. rep. HIGH PRESSURE PHYSICS LABORATORY, University of Oklahoma, 1961.

[3] Lin Hu et al. “Thermal conductivity of tungsten: Effects of plasma-related structural defects from molecular-dynamics simulations”. In: *Applied physics letters* 111 (2017).

[4] M Fujitsuka et al. “Effect of neutron irradiation on thermal diffusivity of tungsten-rhenium alloys”. In: *Journal of Nuclear Materials* 283-287 (2000), pp. 1148–1151.

[5] URL: `https://www.imoa.info/molybdenum/molybdenum-properties.php`.

[6] Denis Rochais et al. “Microscale thermal characterization at temperatures up to 1000°C by photoreflectance microscopy. Application to the characterization of carbon fibres”. In: *Journal of Physics D Applied Physics* 38 (2005).

[7] I V Savchenko et al. “Thermal conductivity and thermal diffusivity of tantalum in the temperature range from 293 to 1800 K”. In: *Thermophysics and Aeromechanics* 15.4 (2008).

[8] Mohsin Ali et al. “Experimental and numerical comparison of heat accumulation during laser powder bed fusion of 316L stainless steel”. In: *Progress in Additive Manufacturing volume* 7 (2022), pp. 1071–1083.

[9] Choong S Kim. *THERMOPHYSICAL PROPERTIES OF STAINLESS STEELS*. Tech. rep. ARGONNE NATIONAL LABORATORY, 1975.

[10] James H VanSant. *Conduction Heat Transfer Solutions*. 1980.

[11] WJ Parker et al. “Flash Method of Determining Thermal Diffusivity, Heat Capacity, and Thermal Conductivity”. In: *Journal of Applied Physics* 32 (1961).

[12] Y S Touloukian et al. *Thermophysical properties of matter - the TPRC data series*. Vol. 1. 1970. URL: `https://www.osti.gov/biblio/5447756`.

[13] A V Khvan et al. “Thermodynamic properties of tin: Part I Experimental investigation, ab-initio modelling of alpha-, beta-phase and a thermodynamic description for pure metal in solid and liquid state from 0 K”. In: *Calphad* 65 (2019), pp. 50–72.

[14] URL: `https://www.angstromsciences.com/density-elements-chart`.

[15] Josef Stetina et al. “Numerical Model of Heat Transfer and Mass Transfer During the Solidification of a Concasting Steel”. In: *8th Thermal Engineering Joint Conference* (2011).

[16] Kurt E Metzinger. *Hex Element Aspect Ratio and Formulation*. Tech. rep. Sandia National Lab. (SNL-NM), Albuquerque, NM (United States), 2019.

[17] RYO KAWABATA et al. “Solubilities of molybdenum in liquid tin”. In: *Metallurgical and Materials Transactions B* 26 (1995), pp. 654–655.

[18] C. Amy et al. “Pumping liquid metal at high temperatures up to 1673 kelvin”. In: *Nature* 550 (2017), pp. 199–203.

A

Speed of melt front

The working volume of the pump, as designed by [1] has a diameter of 11 mm. The requirement is that 4 ml of liquid tin must be pumped from the low pressure end to the high pressure end of the working volume in one hour.

Using the fact that tin expands by 2.7% on melting, 4 ml of liquid tin is equivalent to about 3.895 ml of solid tin.

$$\text{volume of liquid tin} = 1.027 \times \text{volume of solid tin} \tag{A.1}$$

$$4ml = 1.027 \times \text{volume of solid tin} \tag{A.2}$$

$$\text{volume of solid tin} \approx 3.895ml \tag{A.3}$$

$$\tag{A.4}$$

For a working volume of diameter 11 mm, the length occupied by 3.895 ml of solid tin is

$$\pi \times (5.5)^2 \times length = 3.895 \times 10^3 mm^3 \tag{A.5}$$

$$length \approx 40.986mm \tag{A.6}$$

Hence, for liquid tin to be pumped at a rate of 4 ml/r, solid tin must be consumed at the rate of 40.986 mm/hr. In other words, the solid block of tin in the working volume must move at the rate of 40.986 mm/hr, and so does the melt front.

$$\text{Speed of melt front} = 40.986\text{mm/hr} = 0.683\text{mm/min}$$

B

Other design constraints

Mechanical Constraints

1. Since the system is meant to contain pressurized liquid tin, safety regulations apply to the design of the pump. This means that the pump body must have a certain thickness to withstand the pressure developed. This thickness depends on the pressure levels and the diameter of the tin line, and is referred to as the safe radius. Any accessories of the pump must be placed outside this safe radius.
2. The pump body is not perfectly rigid, and there is always some expansion of the material both due to mechanical and thermal effects. Hence there is some room for tin to expand, leading to pressure loss.
3. Liquid tin is not a perfectly incompressible fluid, so the maximum possible pressures are not achieved on melting.
4. The solid tin in the tin line is not a good rigid wall to contain pressurized liquid tin. Solid tin in contact with pressurized liquid tin is subject to effects like melting, plastic deformation, extrusion, etc.

Material Constraints

Liquid tin is aggressive towards most metals it contacts. Since the pump body must be made out of a thermally conducting material, the options for materials are limited. Some thermally conductive materials that are also resistant to attack by Tin are W, Mo, hard-inchromized stainless steel [17, 18]. Other materials that are unaffected by liquid Tin include graphite, refractory ceramics like Al_2O_3, AlN, SiC and ZrO_2 [18].

C Results of parameter study

For a pump configuration with chosen design parameters, the possibility of achieving a steady state thermal gradient between adjacent zones is evaluated using the inverse gain matrix (section 5.4.3). If the input heater Powers required in order to achieve the gradient are negative, it shows that either the amount of heat extracted by the sink is insufficient (low sink contact area) or the crosstalk between the adjacent zones is too high (small zone length). This means that the chosen configuration will not work.

C.1. L = 50 mm, A = 45$\times$25 mm^2

	TSn1	TSn2	TSn3	TSn4
H1	1.91	1.39	1.01	0.84
H2	1.44	1.52	1.15	0.95
H3	1.03	1.2	1.46	1.27
H4	0.84	0.97	1.28	1.75

Figure C.1: Gain matrix

1.71	-1.67	0.16	-0.03
-1.88	3.59	-1.68	0.17
0.40	-2.03	3.33	-1.50
-0.07	0.30	-1.58	1.59

Figure C.2: Inverse gain matrix

For the following tin temperatures across the zones,

$$[T] = \begin{bmatrix} 200 \\ 200 \\ 250 \\ 250 \end{bmatrix}$$

the required input powers of the heaters are:

$$[P] = G^{-1} \times [T] = \begin{bmatrix} 40 \\ -35 \\ 130 \\ 48 \end{bmatrix}$$

C.2. L = 50 mm, A = 65×35 mm^2

	TSn1	TSn2	TSn3	TSn4
H1	1.45	0.96	0.62	0.48
H2	1.01	1.09	0.74	0.57
H3	0.63	0.78	1.04	0.86
H4	0.48	0.59	0.87	1.33

Figure C.3: Gain matrix

1.77	-1.62	0.11	-0.01
-1.85	3.60	-1.59	0.14
0.36	-1.94	3.35	-1.46
-0.05	0.25	-1.53	1.65

Figure C.4: Inverse gain matrix

For the following tin temperatures across the zones,

$$[T] = \begin{bmatrix} 200 \\ 200 \\ 250 \\ 250 \end{bmatrix}$$

the required input powers of the heaters are:

$$[P] = G^{-1} \times [T] = \begin{bmatrix} 54.91 \\ -12.22 \\ 158.02 \\ 70.74 \end{bmatrix}$$

C.3. L = 50 mm, A = 65×40 mm^2

	TSn1	TSn2	TSn3	TSn4
H1	0.82	0.40	0.18	0.10
H2	0.44	0.55	0.26	0.15
H3	0.18	0.29	0.51	0.34
H4	0.10	0.16	0.35	0.74

Figure C.5: Gain matrix

2.04	-1.55	0.11	-0.01
-1.79	3.92	-1.49	0.13
0.33	-1.85	3.73	-1.38
-0.04	0.23	-1.44	1.97

Figure C.6: Inverse gain matrix

For the following tin temperatures across the zones,

$$[T] = \begin{bmatrix} 200 \\ 200 \\ 250 \\ 250 \end{bmatrix}$$

the required input powers of the heaters are:

$$[P] = G^{-1} \times [T] = \begin{bmatrix} 121.19 \\ 85.45 \\ 284.22 \\ 169.88 \end{bmatrix}$$

In this configuration, the required heater powers are non-negative, which means that is is possible to create a gradient of 50 K. However, the heater powers are far higher than 100 W, which is the maximum power limit per heater.

C.4. L = 140 mm, A = 45×25 mm^2

	TSn1	TSn2	TSn3	TSn4
H1	1.70	0.89	0.48	0.32
H2	0.90	1.21	0.69	0.46
H3	0.48	0.69	1.19	0.83
H4	0.32	0.46	0.84	1.57

Figure C.7: Gain matrix

0.97	-0.74	0.04	0.00
-0.75	1.81	-0.77	0.03
0.04	-0.79	1.81	-0.74
0.00	0.05	-0.75	1.02

Figure C.8: Inverse gain matrix

For the following tin temperatures across the zones,

$$[T] = \begin{bmatrix} 200 \\ 200 \\ 250 \\ 250 \end{bmatrix}$$

the required input powers of the heaters are:

$$[P] = G^{-1} \times [T] = \begin{bmatrix} 55.42 \\ 28.52 \\ 118.66 \\ 75.07 \end{bmatrix}$$

In this configuration, the required heater powers are non-negative, and also the maximum required power is close to 100 W.

C.5. L = 140 mm, A = 65×35 mm^2

	TSn1	TSn2	TSn3	TSn4
H1	1.40	0.67	0.32	0.19
H2	0.67	0.99	0.50	0.30
H3	0.32	0.51	0.97	0.63
H4	0.19	0.30	0.64	1.31

Figure C.9: Gain matrix

1.06	-0.74	0.04	0.00
-0.74	1.90	-0.77	0.03
0.04	-0.79	1.90	-0.73
0.00	0.05	-0.75	1.11

Figure C.10: Inverse gain matrix

For the following tin temperatures across the zones,

$$[T] = \begin{bmatrix} 200 \\ 200 \\ 250 \\ 250 \end{bmatrix}$$

the required input powers of the heaters are:

$$[P] = G^{-1} \times [T] = \begin{bmatrix} 74.01 \\ 48.66 \\ 142.52 \\ 99.87 \end{bmatrix}$$

C.6. L = 140 mm, A = 65×40 mm^2

	TSn1	TSn2	TSn3	TSn4
H1	1.26	0.37	0.10	0.04
H2	0.37	0.79	0.25	0.10
H3	0.10	0.25	0.78	0.34
H4	0.04	0.10	0.34	1.17

Figure C.11: Gain matrix

0.92	-0.44	0.02	0.00
-0.44	1.62	-0.47	0.01
0.02	-0.47	1.62	-0.43
0.00	0.01	-0.43	0.98

Figure C.12: Inverse gain matrix

For the following tin temperatures across the zones,

$$[T] = \begin{bmatrix} 200 \\ 200 \\ 250 \\ 250 \end{bmatrix}$$

the required input powers of the heaters are:

$$[P] = G^{-1} \times [T] = \begin{bmatrix} 101.99 \\ 122.07 \\ 207.53 \\ 139.45 \end{bmatrix}$$